NASA TN D-54

TECHNICAL NOTE
D-54

SHOCK-TUBE HEAT-TRANSFER MEASUREMENTS ON INNER SURFACE OF A CYLINDER (SIMULATING A FLAT PLATE) FOR STAGNATION-TEMPERATURE RANGE 4,100° TO 8,300° R

By Jim J. Jones

Langley Research Center
Langley Field, Va.

NATIONAL AERONAUTICS AND SPACE ADMINISTRATION

WASHINGTON September 1959

NATIONAL AERONAUTICS AND SPACE ADMINISTRATION

TECHNICAL NOTE D-54

SHOCK-TUBE HEAT-TRANSFER MEASUREMENTS ON INNER SURFACE OF A CYLINDER (SIMULATING A FLAT PLATE) FOR STAGNATION-TEMPERATURE RANGE 4,100° TO 8,300° R

By Jim J. Jones

SUMMARY

A shock-tube investigation has been made of the heat-transfer rate to the inner surface of a hollow cylinder. The Reynolds number range was from approximately 2×10^5 to 2×10^7. The Mach number range was from about 1.8 to 2.4. The stagnation-temperature range was from 4,100° to 8,300° R.

The turbulent results could be correlated with a curve similar in form to the classical incompressible relation, except that the heat-transfer parameter was based on enthalpy rather than temperature.

Very little laminar-boundary-layer data were obtained. Boundary-layer transition occurred at a Reynolds number of about 5×10^5.

INTRODUCTION

Turbulent boundary layer may well exist over a large portion of a hypersonic vehicle for some flight conditions and the expected heating rate must therefore be calculated on the basis of turbulent flow. However, lack of understanding of the fundamental structure of turbulence has made it necessary to rely on empirical relations for estimating skin friction and heat-transfer rate. For hypersonic flight speeds, the real-gas effects introduce new uncertainties into the problem.

Only a very limited amount of heat-transfer data has been obtained in the real-gas regime. In reference 1 an approximate analysis is presented for turbulent flow in a partially dissociated gas with the effects of atomic diffusion included. Since that analysis was intended primarily for studying the reentry of a blunt-nosed body, where the local Mach number would be much less than the free-stream Mach number, it is essentially an incompressible analysis. The resulting heat-transfer equation for the case of a flat plate, in terms of the Nusselt number N_{Nu}, Reynolds

number N_{Re}, and Prandtl number N_{Pr}, is (free-stream conditions denoted by subscript ∞)

$$\left(N_{Nu}\right)_{\text{real gas}} = 0.029\left[1 + \left(N_{Le}^{\beta} - 1\right)\frac{h_{d,\infty}}{h_{t,\infty}}\right]N_{Re,\infty}^{0.8}N_{Pr,\infty}^{1/3}$$

This relation differs from the classical incompressible relation for turbulent flow in that a term (in brackets) involving the Lewis number N_{Le} to some power β and the fraction of the total enthalpy in dissociation in the free stream $\frac{h_{d,\infty}}{h_{t,\infty}}$ is included to account for the effects of atomic diffusion. One other important difference is that the Nusselt number is based on enthalpy rather than temperature as the driving potential. The free-stream stagnation enthalpy is used as the recovery enthalpy in reference 1. For conditions similar to those of the present tests in which the local Mach number is low and the wall enthalpy is small compared with the total enthalpy, the assumption of a recovery factor of, say 0.9, would increase the Nusselt number by less than 5 percent.

Reference 1 also presented heat-transfer measurements, obtained in a shock tube, on the cylindrical portion of a hemisphere-cylinder model. The results correlated fairly well with the incompressible relation (using enthalpy as the driving potential), which requires that $N_{Le}^{\beta} = 1$. It was shown, however, that a slightly better correlation could be obtained for $N_{Le}^{\beta} = 1.4$.

In the present investigation, heat-transfer measurements were made in the high-pressure shock tube in the Langley gas dynamics laboratory on the inner surface of a glass cylinder which was axially alined with the flow. Since the leading edge was sharp and the boundary-layer displacement thickness was estimated to be only about 3 to 4 percent of the radius of the cylinder at the downstream end, the pressure gradient was small and was neglected. Thus, the fundamental difference between this model and that of reference 1 is the absence of a strong bow shock wave for the present case.

The Reynolds number range of these tests, based on x and local-stream conditions, was from about 2×10^5 to 2×10^7. Since the tests were conducted in a constant-area shock tube, the Mach number varied from about 1.8 to 2.4. The stagnation-temperature range of the tests (4,100° to 8,300° R) corresponds to that encountered in flight at

100,000 feet for the Mach number range of 7 to 14. The degree of dissociation was small; however, the stream conditions are shown to be applicable to practical flight conditions.

SYMBOLS

c_p specific heat at constant pressure, $\frac{\text{Btu}}{\text{Slug-}^{\circ}\text{R}}$

c_w specific heat of wall material, $\frac{\text{Btu}}{\text{Slug-}^{\circ}\text{R}}$

D diffusion coefficient, $\frac{\text{sq ft}}{\text{sec}}$

h enthalpy, $\frac{\text{Btu}}{\text{slug}}$

$\frac{h_{d,\infty}}{h_{t,\infty}}$ fraction of total enthalpy in dissociation in free stream

k thermal conductivity, $\frac{\text{Btu}}{(\text{sec})(\text{ft})(^{\circ}\text{R})}$

N_{Le} Lewis number, $\frac{D\rho c_p}{k}$

M Mach number

N_{Nu} Nusselt number, $\frac{qxN_{Pr,\infty}}{\mu_{\infty}(h_{t,\infty} - h_w)}$

N_{Pr} Prandtl number, $\frac{c_p\mu}{k}$

N_{Re} Reynolds number, $\frac{\rho Vx}{\mu}$

p static pressure, $\frac{\text{lb}}{\text{sq in.}}$ abs

q	heat-transfer rate, $\frac{\text{Btu}}{(\text{sq ft})(\text{sec})}$
T	temperature, $^{\circ}R$
ΔT	temperature rise of model surface, $T_w - T_{w,\text{initial}}$, $^{\circ}R$
V	velocity, ft/sec
x	distance along cylinder axis from leading edge, ft unless otherwise indicated
β	power of Lewis number in heat-transfer equation
λ	variable of integration in equation (1)
μ	viscosity, $\frac{\text{Slugs}}{\text{ft-sec}}$
ρ	density, $\frac{\text{Slugs}}{\text{cu ft}}$
τ	time after shock passage, sec
$( )'$	properties based on reference enthalpy

Subscripts:

g	glass-model properties
r	recovery, or adiabatic wall condition
s	shock-wave conditions
t	total, or stagnation conditions
w	wall conditions
∞	local-stream conditions just outside boundary layer

In this paper, the local-stream conditions are assumed to be the same as the conditions immediately behind the primary (moving) shock wave at the instant it passes over the model.

APPARATUS

The shock tube used for this investigation is the same one described in reference 2. The driver chamber is about 14 feet long and the low-pressure chamber is about 90 feet long. Both chambers are $3\frac{3}{4}$ inches in diameter. The model was mounted approximately 74 feet from the diaphragm station. At the model station the chamber was divided to form a Y-section and the flow exhausted through two tubes downstream of the model station. (See fig. 1.)

The models were Pyrex tubes, 24 inches long, with an outside diameter of 50 millimeters. Five models were tested, differing only in wall thickness and location of measuring stations. The model geometry is summarized in the table shown in figure 1. The wall thickness of the models was increased in an attempt to prevent breakage of the model; however, each of the models was eventually destroyed in testing. Inspection between runs showed no sign of damage prior to the run in which the model was destroyed.

Each of the models had a hardened-steel leading edge which was sharp (less than 0.001 inch blunt) and smoothly joined at the juncture with a glass-to-metal cement.

Three platinum Hanovia paint resistance thermometers (ref. 3) were applied to the inner surface of each model. The strips were about 1/16 inch wide (axial dimension) by 1/2 inch long (circumferential dimension). The thickness was of the order of 10^{-6} inches.

The static-pressure history measurements were made using a quartz-crystal pressure transducer mounted in the wall of the shock tube. Ionization probes were used along with the pressure transducer and thermometer elements to detect the travel of the shock wave.

Both pure hydrogen and a hydrogen-oxygen-helium combustion were used as drivers for these tests. The initial pressure in the low-pressure chamber varied from 10 to 150 millimeters of mercury absolute. The range of shock Mach number was from 4.61 to 8.45 as measured at the model leading edge.

RESULTS AND DISCUSSION

A typical temperature-time history obtained from a resistance thermometer is presented in figure 2. (The circular symbols merely represent

the points at which the oscillograph record was read.) The time of passage of the shock wave across the face of the thermometer element is less than 1 microsecond and therefore essentially instantaneous in the present time scale. Immediately following the passage of the shock wave is a period of unsteady boundary-layer development in which the boundary layer increases its thickness with time. This period appears on the record as an interval of nearly constant surface temperature. This unsteady boundary layer is essentially the same phenomenon as that which occurs on the walls of the shock tube. The unsteady boundary-layer development persists approximately until the particles which were set in motion by the shock wave at the instant it reached the model leading edge have passed over the point of measurement. Thus, the order of magnitude of the unsteady-flow time or "starting" time can be approximated by $x\left(\frac{1}{V_\infty} - \frac{1}{V_s}\right)$. For the sample record shown, the starting time calculated in this manner would be about 20 microseconds. The oscilloscope record indicated the time to be about 35 microseconds.

After the starting process, nearly steady flow exists for the duration of the flow of air over the model. Conditions are not constant during the run because perturbations of the temperature, pressure, and velocity result from the boundary-layer development along the walls of the shock tube. These phenomena are referred to herein as attenuation effects.

It is necessary to obtain the heat-transfer rate from the measured surface-temperature history. This problem is discussed in some detail in reference 3. The solution of the one-dimensional heat-flow equation in a semi-infinite slab (thus, the presence of the thermometer is neglected) gives the heat flux q at any time τ and surface-temperature history $F(\lambda)$ as

$$q = \frac{\sqrt{k_g \rho_g c_{w,g}}}{\pi} \int_0^\tau \frac{\frac{d}{d\lambda} F(\lambda)}{\sqrt{\tau - \lambda}} \, d\lambda \tag{1}$$

where λ is the variable of integration. Reference 3 gives the development of this equation as well as more exact forms to account for the presence of the thermometer. Equation (1) can be written as

$$q = \frac{\sqrt{k_g \rho_g c_{w,g}}}{\pi} \left[\frac{F(\tau)}{\sqrt{\tau}} + \frac{1}{2} \int_0^\tau \frac{F(\tau) - F(\lambda)}{(\tau - \lambda)^{3/2}} \, d\lambda \right] \tag{2}$$

Numerical difficulties are encountered in evaluating the integral as λ approaches τ. The method used herein to avoid these difficulties was to evaluate the integral from 0 to τ_1 where τ_1 was taken as 0.9τ and to assume a straight-line function for $F(\lambda)$ from τ_1 to τ. Thus, equation (2) becomes

$$q = \frac{\sqrt{k_g \rho_g c_{w,g}}}{\pi}\left[\frac{F(\tau)}{\tau} + \frac{1}{2}\int_0^{\tau_1} \frac{F(\tau) - F(\lambda)}{(\tau - \lambda)^{3/2}}\, d\lambda + \frac{F(\tau) - F(\tau_1)}{\sqrt{\tau - \tau_1}}\right] \qquad (3)$$

Rewriting the last term gives

$$q = \frac{\sqrt{k_g \rho_g c_{w,g}}}{\pi}\left[\frac{F(\tau)}{\tau} + \frac{1}{2}\int_0^{\tau_1} \frac{F(\tau) - F(\lambda)}{(\tau - \lambda)^{3/2}}\, d\lambda + \frac{F(\tau) - F(\tau_1)}{\tau - \tau_1}\sqrt{\tau - \tau_1}\right] \qquad (4)$$

If the surface temperature is proportional to the square root of time for the interval τ_1 to τ, the assumption of a linear variation results in an underestimation of q by 4 percent. Thus, if the linear approximation is used and the result is corrected by 4 percent the method becomes very nearly exact.

The experimental heat-transfer rates have been calculated at several values of τ using equation (4). Figure 3 presents the values of q obtained at $\tau = 0.2$, 0.4, 0.6, and 0.8 millisecond for the run shown in figure 2. Figure 3 shows that the heat-transfer rate increases rather rapidly with time, having increased by one-third in 0.8 millisecond. The trend of all the data is for q to increase with time since the attenuation effects result in an increase of pressure and stagnation temperature with time. For a number of the runs the instantaneous values of the flow properties were evaluated approximately at the times for which the heat flux was determined and it was found that all the data correlated on a Nusselt number-Reynolds number basis, within the accuracy of the experiment. Thus, nothing new is added by presenting the data for several values of τ. Because of this and because the flow properties can be evaluated most accurately immediately after shock passage, only data for time $\tau = 0.2$ millisecond are included in this paper.

The heat-transfer data based on stream conditions are presented in figure 4 in the form N_{Nu}/N_{Pr} plotted against N_{Re}. The flow conditions of all the runs are presented in table I. These are stream conditions immediately after shock passage, based on real-gas tables. (See refs. 4 to 6.)

The curves shown for laminar and turbulent boundary-layer flow in figure 4 represent the classical incompressible flat-plate relations, employing the modified Reynolds analogy and using the enthalpy difference as the driving potential. Reference 1 gives for the turbulent boundary layer on a flat plate

$$N_{Nu} = 0.029 N_{Pr}^{1/3} \left[1 + \left(N_{Le}^{\beta} - 1 \right) \frac{h_{d,\infty}}{h_{t,\infty}} \right] N_{Re}^{0.8}$$

where the fluid properties are evaluated just outside the boundary layer. Thus, if the dissociation energy is a negligible part of the total enthalpy, or if $N_{Le}^{\beta} = 1$, the equation is identical with the incompressible form. For the temperature range of the present tests, the quantity $h_{d,\infty}/h_{t,\infty}$ is small - of the order of 0.01. Therefore, the factor N_{Le}^{β} is of little importance in this range and a value cannot be determined from the experiment with any suitable accuracy. The data tend to substantiate the theoretical curve as regards the value of the constant coefficient and the power of the Reynolds number for this range. It may be seen that most of the data points lie within 10 percent of the curve. A few points, however, differ from the theoretical value by as much as 30 percent. Thus, the results are in essential agreement with the data of reference 1 which were obtained on the cylindrical portion of a hemisphere-cylinder.

Only a few points were obtained for a laminar boundary layer. On those runs for which the laminar heating rate was observed, transition to turbulent heating appeared to occur after approximately 0.5 millisecond. This transition was believed to be due to the entrance into the tube of the boundary layer on the shock-tube wall. This boundary layer grows continuously at the model station during the period of the flow of air over the model. Since the runs for which the laminar data were obtained were those runs with the lowest value of Reynolds number per foot, the boundary layer on the shock-tube wall grew the most rapidly. When its thickness was great enough to include the flow entering the model, the turbulence introduced into the model boundary layer could be expected to promote transition.

Transition on the model occurred at a Reynolds number of the order of 5×10^5. This seems to be a low value of transition Reynolds number in comparison with most supersonic wind-tunnel results at similar Mach numbers, although reference 7 reports similarly low transition Reynolds numbers for high boundary-layer cooling rates. However, very little is known about the turbulence level behind a strong shock wave in a shock tube as compared with the turbulence level in a supersonic tunnel or in

free flight. Thus, comparisons of transition Reynolds numbers are of dubious value at the present time.

For practical engineering application the reference-temperature or reference-enthalpy method has proved to be of value. Reference 8 outlines this method and gives the following equation for the reference enthalpy h' (called i^* in ref. 8):

$$h' = h_\infty + 0.5\left(h_w - h_\infty\right) + 0.22\left(h_r - h_\infty\right)$$

For each run of the present investigation the flow properties were evaluated at the temperature corresponding to the reference enthalpy h', and the parameters N_{Nu} and N_{Re} were calculated. The Prandtl number was held constant at a value of 0.71 and, in order to evaluate h_r, the recovery factors were assumed to be equal to $\sqrt{N_{Pr}}$ and $\sqrt[3]{N_{Pr}}$ for laminar and turbulent flow, respectively. The data in the transition region were assumed to have a turbulent recovery factor.

It may be seen in figure 5 that the agreement of data based on the reference temperature with the incompressible turbulent curve is not quite so good as the agreement shown in figure 4 for the free-stream temperature form. The data appear to have shifted away from the curve by about 20 percent, but the scatter of the data is essentially unchanged. The equation for h' was empirically determined, however, for much smaller values of h_∞/h_w, and it would appear that only a slight change in the constants of the equation for h' would adapt it satisfactorily to the present range of h_∞/h_w.

It cannot be tacitly assumed that the gas is in chemical equilibrium for the short times in which heat-transfer data were taken. An estimate of the relaxation time of the oxygen dissociation, based on reference 9, indicates that for $M_s = 8.45$ (upper limit of the present tests) the flow passing over a thermometer element approaches equilibrium in about 30 microseconds. This time is fairly short compared with $\tau = 200$ microseconds for which the heat-transfer rate was determined. The possibility of nonequilibrium gas conditions, however, is not an important factor for these tests because the dissociation is slight, as indicated by the small value of $h_{d,\infty}/h_{t,\infty}$.

APPLICATION TO FLIGHT

The Mach number of the flow produced in a constant-area shock tube is inherently low (see table I) even for those cases where the stagnation temperature is very high. The low Mach number, of course, implies higher static temperatures than those encountered in the atmosphere. Thus, it may not be altogether obvious where data such as that obtained in the present investigation may be applied without large extrapolations of Mach number effect.

One direct application of the data is to a compression surface behind a blunt leading edge. One effect of a blunt leading edge (which is required on hypersonic vehicles to maintain tolerable heat-transfer rates) is to produce a region of flow in the vicinity of the surface which has a higher entropy as a result of the flow having been processed by the near-normal portion of the bow shock wave. (See ref. 10.) The presence of this shock layer means that the boundary layer develops in a region of reduced Mach number and elevated static temperature as compared with that on the sharp-leading-edge configuration.

If a blunted, two-dimensional wedge is used as a simplified example, conditions may be selected so that the flow over the wedge is similar to the flow conditions of one test of the present investigation. For the test selected, the flow conditions may be compared with those on an 8° half-angle wedge having a blunt leading edge and flying at $M = 13.5$ at an altitude of 70,000 feet. The flow conditions in the shock layer just outside the boundary layer, some distance from the leading edge, are presented for the wedge with corresponding conditions for the test selected in the following table:

Flow conditions	Present investigation	8° half-angle wedge
M_∞	2.40	2.46
T_∞, $^\circ R$	5,690	5,760
p_∞, lb/sq in. abs	9.53	10.3
T_t, $^\circ R$	8,280	8,280
p_t, lb/sq in. abs	181	162

The agreement could be improved by selecting the flight conditions more precisely. The example shows that the conditions of the present tests are within the range of practical interest.

CONCLUDING REMARKS

A shock-tube investigation has been made of the heat-transfer rate to the inner surface of a hollow cylinder. The stagnation-temperature range of the tests was from 4,100° to 8,300° R. The Reynolds number range was from approximately 2×10^5 to 2×10^7 and the Mach number range was from about 1.8 to 2.4.

The results indicate that the classical incompressible relation, with the modified Reynolds analogy, adequately predicts the turbulent heat-transfer rate for this range if the difference between stagnation enthalpy and wall enthalpy is taken as the driving potential. The agreement was not so good when the flow properties were based on the temperature corresponding to reference enthalpy.

Very little laminar-boundary-layer data were obtained in these tests. Transition to turbulent flow occurred at a Reynolds number of about 5×10^5. In those tests in which a thermometer element indicated laminar flow initially after shock passage, transition to a turbulent heating rate occurred in about 0.5 millisecond. This transition was apparently due to the boundary layer on the shock-tube wall having grown to a thickness sufficient to include the flow entering the model.

Langley Research Center,
National Aeronautics and Space Administration,
Langley Field, Va., July 9, 1959.

REFERENCES

1. Rose, Peter H., Probstein, Ronald F., and Adams, Mac C.: Turbulent Heat Transfer Through a Highly Cooled Partially Dissociated Boundary Layer. Res. Rep. 14, AVCO Res. Lab., Jan. 1958.

2. Jones, Jim J.: Experimental Investigation of Attenuation of Strong Shock Waves in a Shock Tube With Hydrogen and Helium as Driver Gases. NACA TN 4072, 1957.

3. Vidal, Robert J.: A Resistance Thermometer for Transient Surface Temperature Measurements. Presented at the Am. Rocket Soc. Meeting (Buffalo), Sept. 24-26, 1956.

4. Hilsenrath, Joseph, Beckett, Charles W., et al.: Tables of Thermal Properties of Gases. NBS Cir. 564, U. S. Dept. Commerce, 1955.

5. Logan, J. G., Jr.: Thermodynamic Charts for High Temperature Air Calculations. (2,000° K to 9,000° K). Rep. No. AD-1052-A-3, (Contract No. AF 40(600)-6, AF 18(603)-10), Cornell Aero. Lab., Inc., July 1956.

6. McKowen, Paul: The Equilibrium Composition and Flow Variables for Air Dissociated by a Strong Shock Wave. Rep. No. 02-984-040, Bell Aircraft Corp., Mar. 8, 1957.

7. Jack, John R., Wisniewski, Richard J., and Diaconis, N. S.: Effects of Extreme Surface Cooling on Boundary-Layer Transition. NACA TN 4094, 1957.

8. Eckert, Ernst R. G.: Survey on Heat Transfer at High Speeds. WADC Tech. Rep. 54-70, Wright Air Dev. Center, U. S. Air Force, Apr. 1954.

9. Camac, M., Camm, J., Keck, J., and Petty, C.: Relaxation Phenomena in Air Between 3000 and 8000° K. Res. Rep. 22, (Contract AF 04(645)-18), AVCO Res. Lab., Mar. 1958.

10. Moeckel, W. E.: Some Effects of Bluntness on Boundary-Layer Transition and Heat Transfer at Supersonic Speeds. NACA Rep. 1312, 1957. (Supersedes NACA TN 3653.)

TABLE I.- FLOW CONDITIONS OF THE TESTS

Model	M_s	M_∞	p_∞, lb/sq in. abs	T_∞, $^\circ R$	$\frac{h_\infty}{h_w}$	T_t, $^\circ R$
1	5.20	1.83	30.3	3,112	6.03	4,590
1	5.50	1.89	33.9	3,400	6.72	4,710
2	6.05	1.98	16.0	3,790	7.56	5,600
2	6.25	2.01	17.0	3,868	7.76	5,720
2	5.63	1.91	21.4	3,425	6.73	5,130
3	7.45	2.23	13.1	5,042	11.26	7,128
3	7.00	2.15	17.1	4,669	9.97	6,516
3	6.17	2.01	26.5	3,978	8.06	5,815
3	5.71	1.92	38.1	3,430	6.74	5,060
3	5.64	1.90	37.0	3,367	6.59	4,930
3	4.93	1.79	54.4	2,830	5.34	4,140
3	4.93	1.79	54.4	2,800	5.32	4,120
4	6.70	2.10	15.25	4,440	9.27	6,660
4	6.95	2.14	17.35	4,700	10.03	6,700
4	7.70	2.27	13.96	5,285	12.28	7,520
4	7.50	2.23	10.4	5,220	12.07	7,250
4	8.45	2.40	9.53	5,690	14.7	8,280
5	6.60	2.04	20.3	4,370	9.05	6,120
5	7.91	2.31	14.9	5,305	12.42	7,525
5	8.10	2.33	14.4	5,380	12.83	7,700
5	8.04	2.27	76.1	5,670	13.12	8,300
5	6.66	2.06	51.5	4,505	9.45	6,510
5	6.72	2.08	78.6	4,585	9.70	6,700
5	5.68	1.91	74.6	3,530	6.98	5,240
5	4.61	1.75	72.6	2,550	4.81	3,760
5	6.88	2.10	109.4	4,605	10.19	6,820

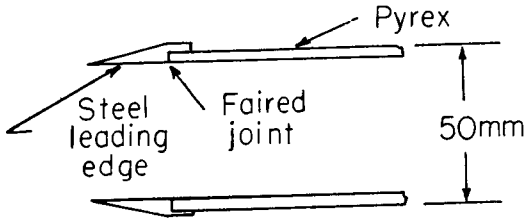

Leading-edge detail

Model	Wall thickness, mm	Thermometer stations, inches from leading edge		
1	2	6.50	12.50	18.50
2	2	6.50	12.50	18.50
3	4	2.75	10.75	18.75
4	4	4.75	12.75	20.75
5	4	6.75	14.75	22.75

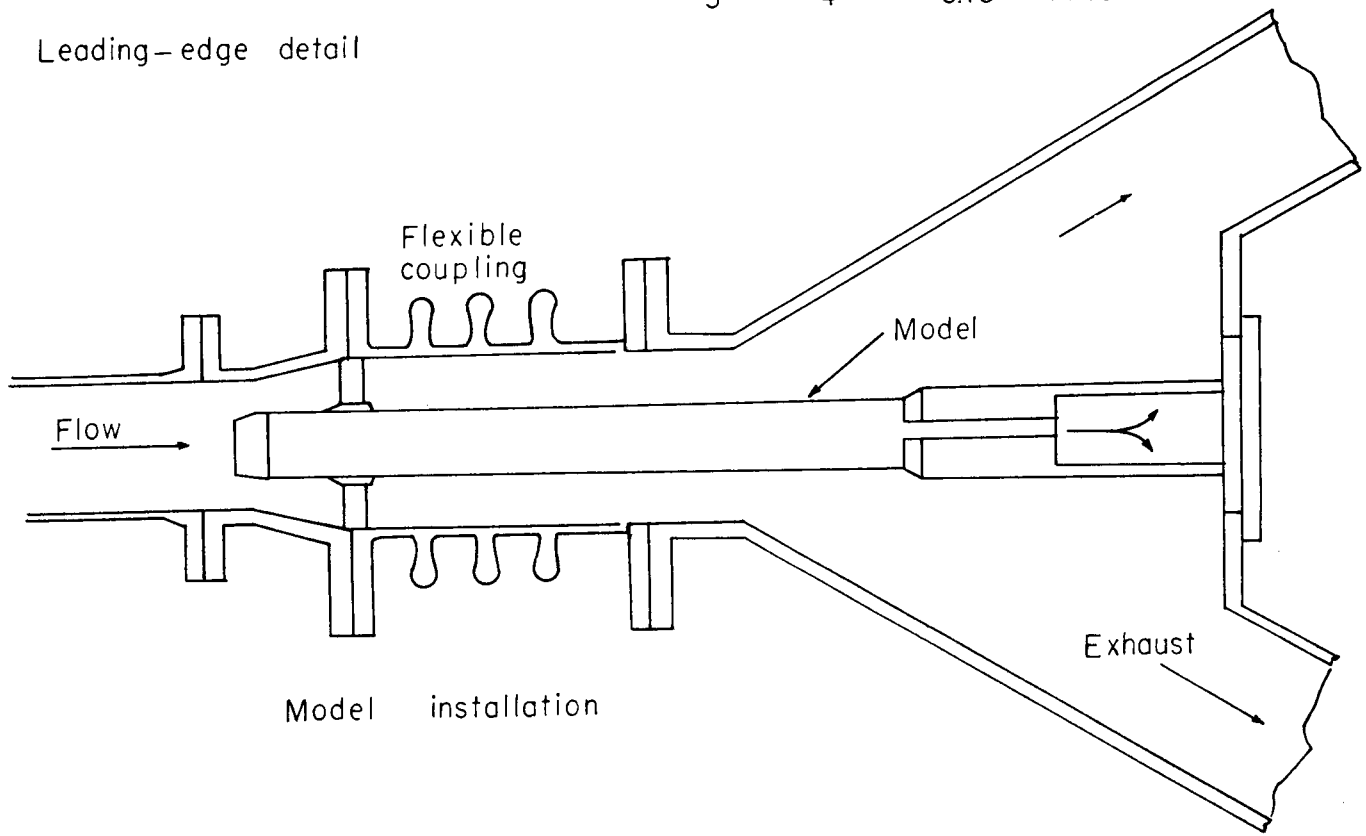

Model installation

Figure 1.- Sketch of model and installation.

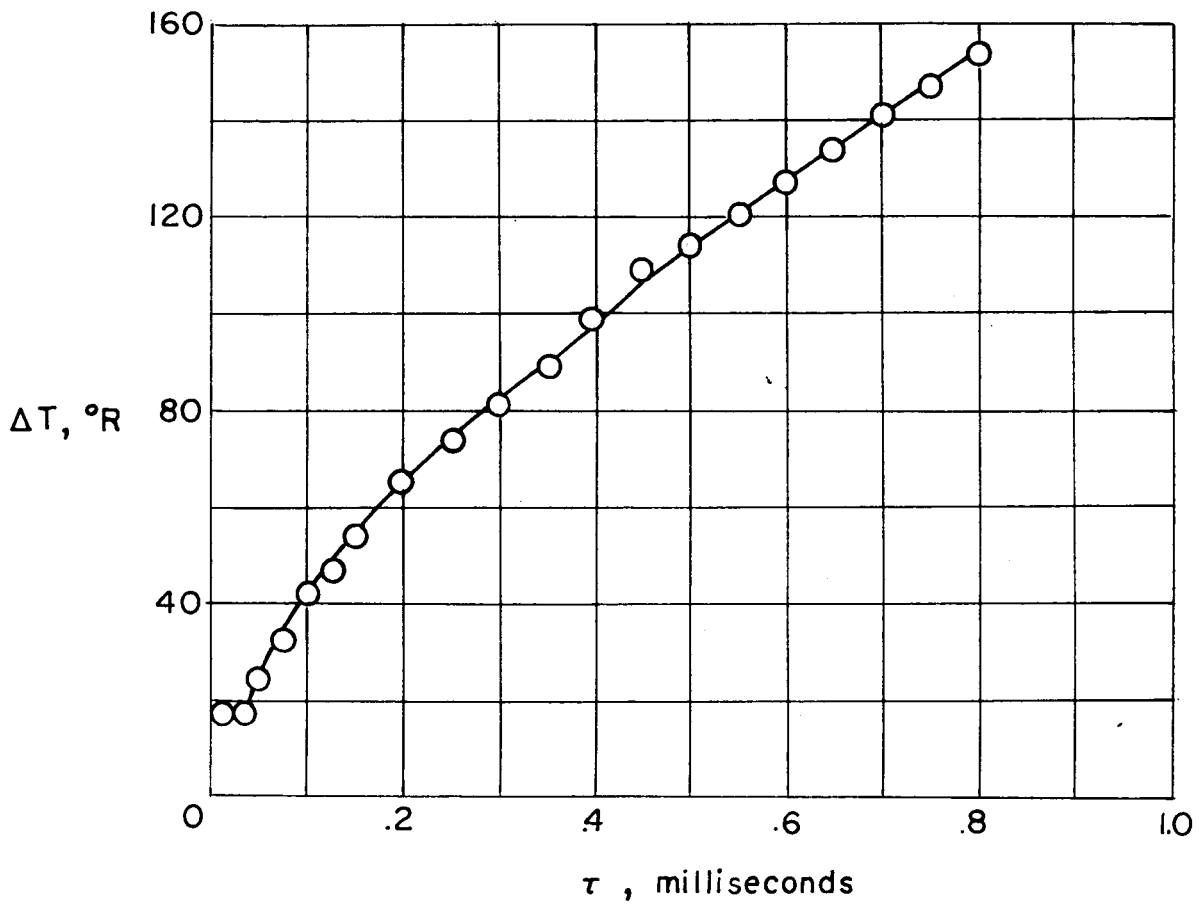

Figure 2.- Typical thermometer output during a run.

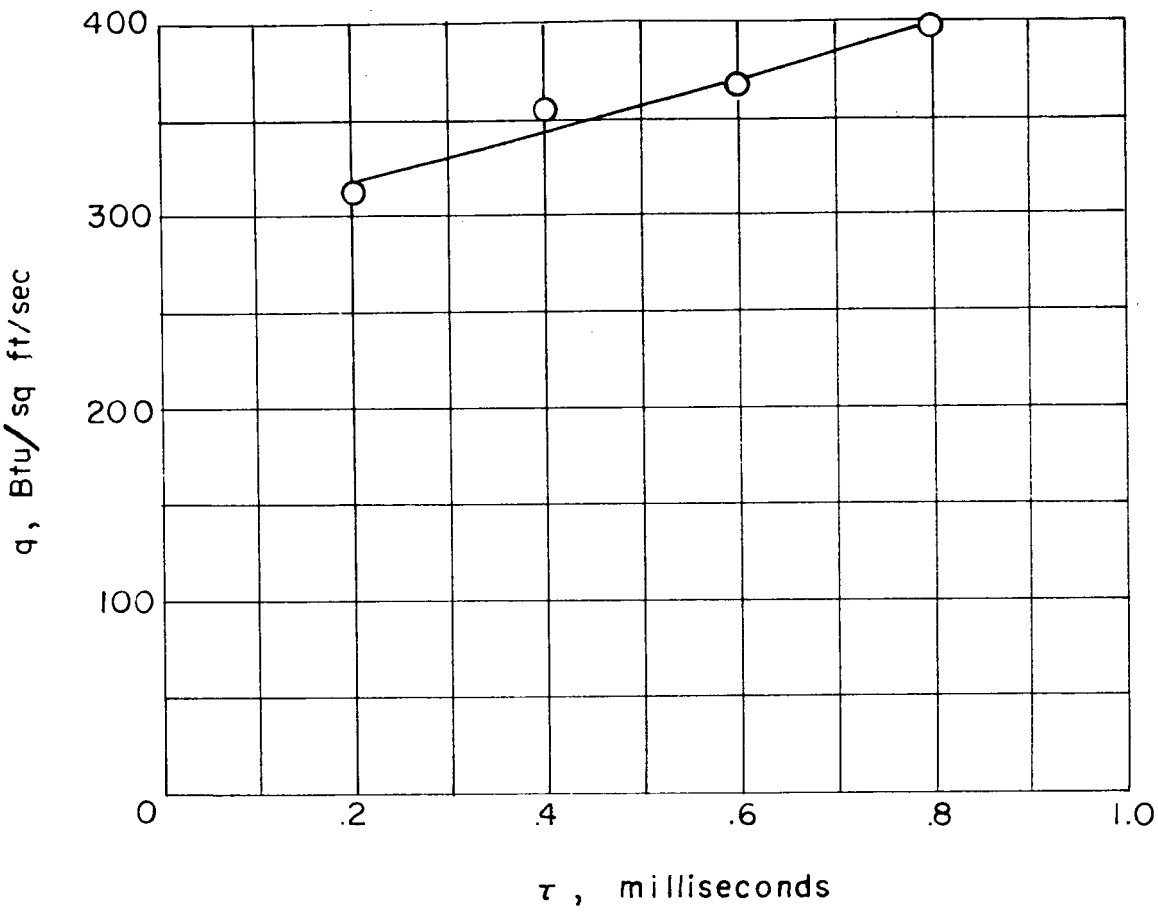

Figure 3.- Time variation of heating rate during a run.

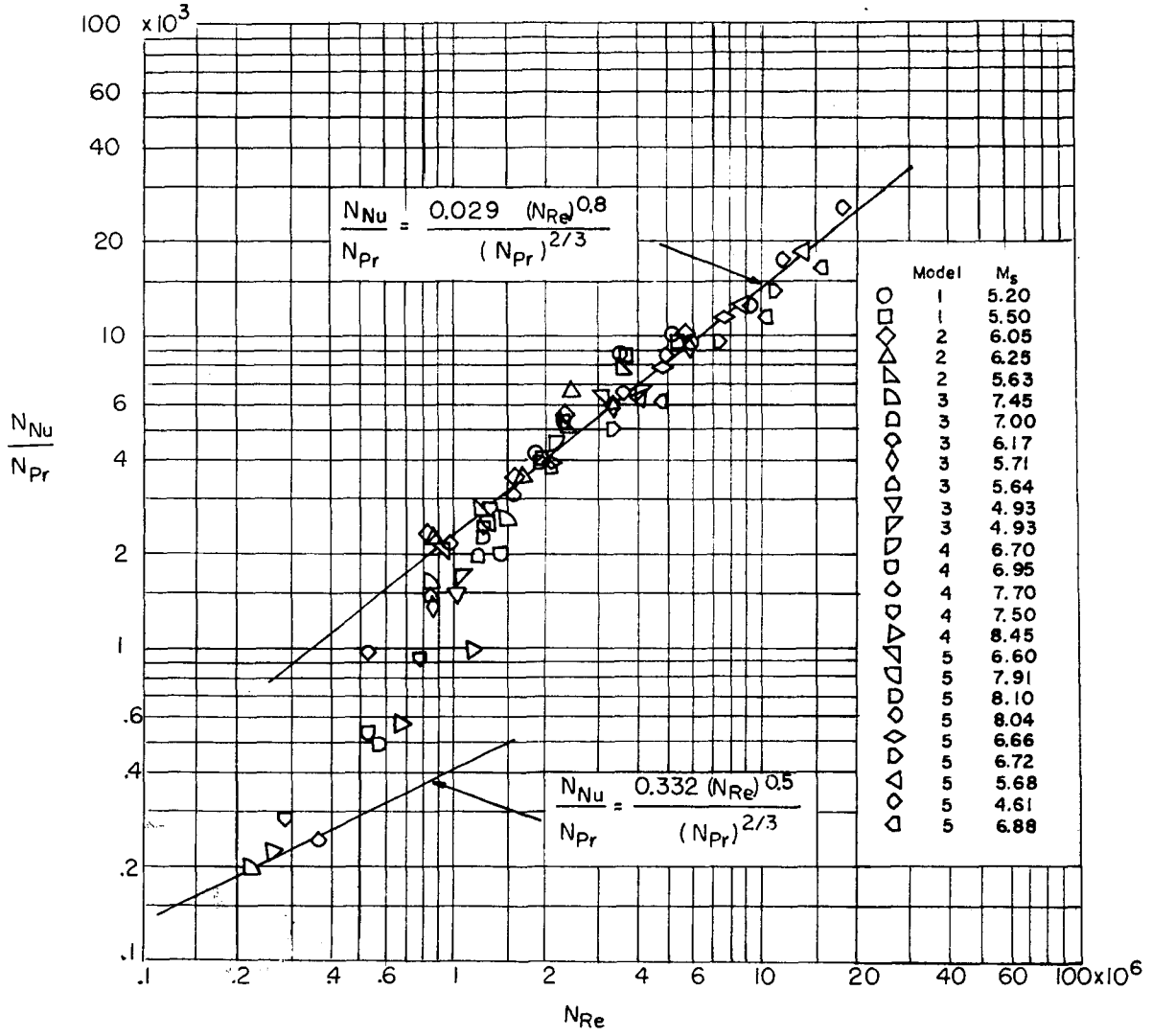

Figure 4.- Heat-transfer data based on stream conditions.

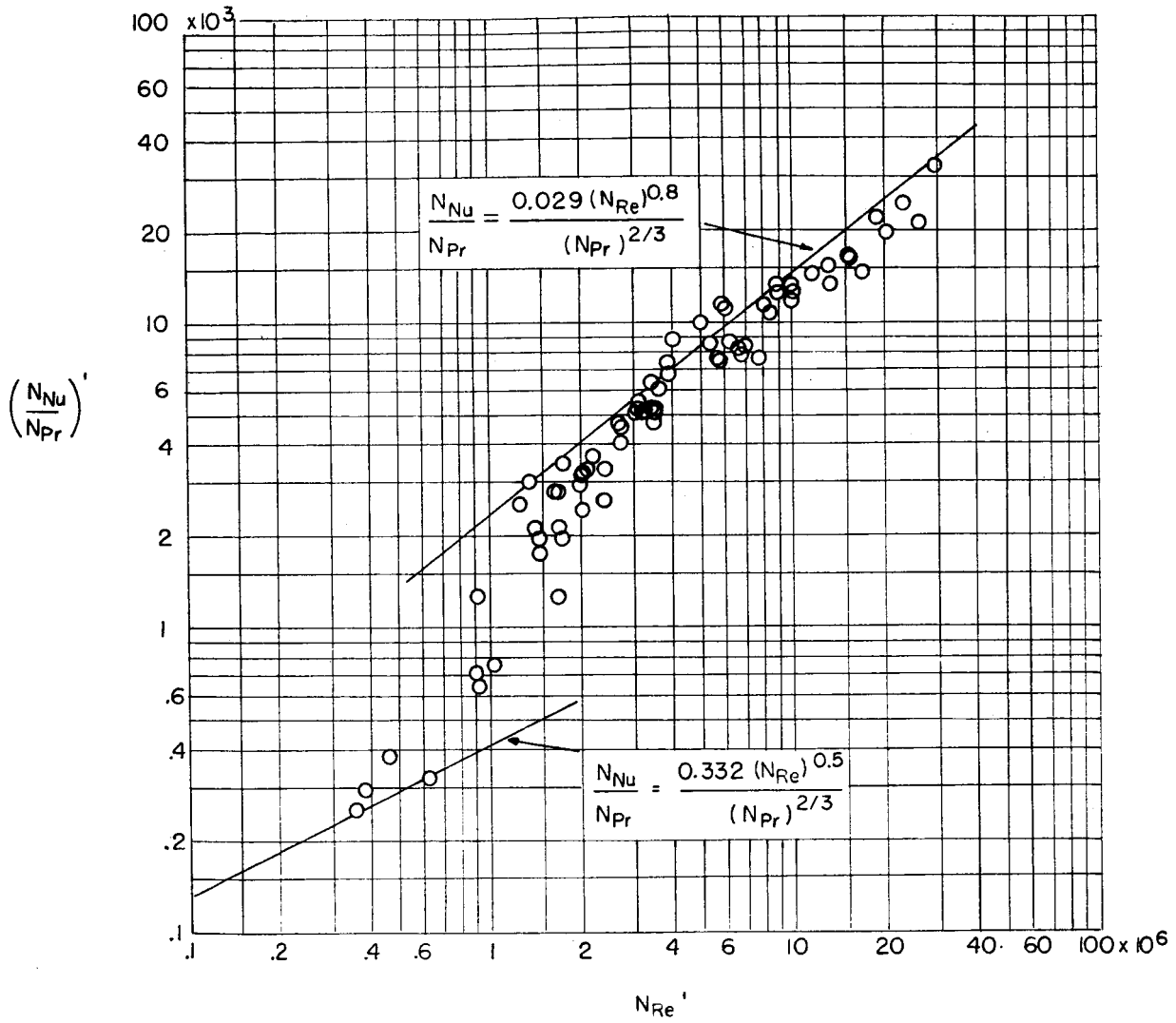

Figure 5.- Heat-transfer data based on reference enthalpy h'.